

Sediment pollution: An assessment of anthropogenic and geogenic trace elements contributions along the central Algerian coast

Mohamed AROUA ^{a,*}, Mostefa BOULAHDID ^a, Olivier RADAKOVITCH ^b, Moustafa BENHALIMA ^{a,c}, Yassine GUENDOUIZI ^c, Scott W. FOWLER ^{d,1}, Jean-Paul AMBROSI ^e

^a Laboratory of Marine and Coastal Ecosystems (ECOSYSMarL), National Higher School of Marine Sciences and Coastal Management (ENSSMAL), BP19, university Campus of Dely Ibrahim, Bois des Cars, 16320, Cheraga, Algiers, Algeria.

^b Institut de Radioprotection et de Surêté Nucléaire (IRSN), PSE/SRTE/LRTA, BP3, 13115, Saint-Paul-Lez-Durance, France.

^c Laboratory Management and Valorization of Agricultural and Aquatic Ecosystems, Science Institute, University Center of Tipaza Morsli Abdallah, Oued Merzoug 42200, Tipaza, Algeria.

^d School of Marine and Atmospheric Sciences, Stony Brook University, Stony Brook, NY 11794-5000, USA

^e Aix-Marseille University., CNRS, IRD, INRA, Coll France, CEREGE, Aix-en-Provence, France. aroua@outlook.be

* *Corresponding author:* aroua@outlook.be

¹ *Present address:* Institute Bobby, 8 Allee des Orangers, 06320 Cap d'Ail, France.

1 **1. Introduction**

2 Trace metals in coastal sediment originating from anthropogenic sources are of increasing interest
3 and concern in modern human society. Due to their stability, bioaccumulative nature, persistence, and
4 their various forms of toxicity in the environment (Inal et al., 2018; Gao et al., 2015), metals can
5 affect the quality of the coastal ecosystems and present a considerable risk to the aquatic organisms
6 and human health (Abderrahmani et al., 2021; Guendouzi et al., 2020). Following their release in the
7 catchment areas from various sources, metals are usually transported through the river system to the
8 coastal zone in dissolved form or bound to suspended particles (Benhalima et al., 2022). Historically,
9 trace metals in the coastal areas are predominantly from the continental weathering of rocks and soil
10 materials (Viers et al., 2009). However, an additional fraction of metals discharged from land-based
11 activities, such as mining and various industrial and agricultural activities, may contribute to the
12 contamination of marine sediments (Barron et al., 2022; Belhadj et al., 2017; Sbarbati et al., 2020).
13 To evaluate the potential contamination of sediment, the man-induced accumulation should be
14 distinguished from the natural background values (Esen et al., 2010). Sediment cores from the coastal
15 zone have been shown to be excellent indicators for the investigation of depositional trends, sources
16 and risk of trace metals (Li and Li, 2017). Many researchers have studied geochemistry and the
17 environmental quality of sediment cores in various aquatic ecosystems globally (Barbieri et al., 2018;
18 Gao et al., 2016; Moushmi et al., 2022; Romano et al., 2018; Zhu et al., 2017).
19 Like many Mediterranean countries, Algeria is facing various environmental challenges in recent
20 years. Among them, the increase in population and their activities in the coastal zone (Khelil et al.,
21 2019). Algeria has a traditional agricultural and oil production-based economy, but with a short
22 history of industrialization and urbanization compared to the developed countries, which makes it a
23 desired area for fieldwork to provide valuable geochemical information on anthropogenic impacts. In
24 fact, Algeria experienced an industrial and agricultural renaissance only in the 1970s after its
25 independence in 1962 and then started an economic recovery after the end of the civil war in 1999,

26 with rapid agricultural development during the last two decades. Agricultural activity has therefore
27 intensified in response to the rapid increase in population, which has increased by 100 % over the last
28 thirty-five years, from 22 million inhabitants in 1985 to 40.4 million in 2015 (Guendouzi et al., 2020)
29 up to 44 million in 2021. Additionally, the Mediterranean climate that characterized the northern
30 country has led to mass population displacement to coastal towns. As a result, the coastal territory
31 concentrates by itself about 45 % of the population, which represents only 1.9 % of the country's total
32 territory (Chemrouk and Chabbi, 2016). This situation exerts great pressure on the coastal ecosystems
33 adjacent to populated areas (Inal et al., 2018).

34 Despite these aspects, there were some studies on trace element distribution in the Algerian coastal
35 sediments. These studies have focused on the spatial distribution of trace elements in surficial
36 sediments (Inal et al., 2018; Bachouche et al., 2017; Belhadj et al., 2017; Kouidri et al., 2016);
37 however, trace metal investigations in sediment cores are rarely studied. Hence, the major purposes
38 of this research were (1) to investigate the distribution of trace metals on the central Algerian coast,
39 (2) to analyze the depositional behavior and origin of trace metals through multi-statistical analyses,
40 and (3) to assess the degree of the metal enrichment and the potential sediment toxicity. The results
41 obtained in this work may provide baseline data for the present and future assessment of
42 environmental risks associated with the occurrence of trace metals to implement coastal zone
43 management strategies.

44 **2. Materials and methods**

45 **2.1. Study area**

46 Located in the southwestern part of the Mediterranean Sea, Algeria's coastline extends about 1622
47 km and includes fourteen coastal cities. On the central coast, three towns, namely Algiers,
48 Boumerdes, and Tipasa are exceptional cases of urban expansion areas where land-based and sea
49 activities have intensified in recent years. Most previous studies were limited to Algiers which is

50 considered the most industrialized in the country. This city hosts the most important industrial zones
51 in the country, among which are the Oued Samar and Baba Ali industrial zones, where factories
52 constantly discharge untreated effluent into Algiers bay via El Harrach river (Fouzia et al., 2013). On
53 the other hand, the inner part of Algiers Bay contains paper and iron factories, chemical and textile
54 industries, desalination plants, metal processing, food and beverage manufacturing, tanneries and oil
55 (Bachouche et al., 2017). Additionally, the port of Algiers which is located in the western part of the
56 bay hosts some of such industries, as well as oil refinery plant and petrochemical factory, which
57 impact the adjacent marine environment (Taieb-Errahmani et al., 2020). The Intensive maritime
58 traffic and urban wastes in the capital are the other factors that influence sediment quality. Unlike
59 Algiers, Tipaza and Boumerdes are regarded as agricultural and tourist zones vocation. In addition to
60 agricultural amendments plants, and fertilizer factories that characterized the areas, several industrial
61 infrastructures have been developed on the coast to meet the growing need for drinking water and
62 energy like seawater desalination plants of Fouka (Tipasa) and thermal power station of cap Djinet
63 (Boumerdes) (Khelil et al., 2019). A recent study reported that the most polluted sediments along the
64 Algerian coastline are located on the central coast (Inal et al., 2018); thus, it is of great interest to
65 evaluate the impact of human activities on this particular marine environment. Furthermore, several
66 rivers are discharged along the central marine coastline (Inal et al., 2018), the most important being
67 El Harrach river entering into Algiers Bay, the Nador river in Bou Ismail Bay, and the Isser river
68 entering Zemmouri Bay (Fig.1). The rivers drain mainly urban and agricultural areas and their
69 hydrological regime is very variable characterized by temporary flows following generally the rainfall
70 contributions (Karahacane et al., 2020). According to meteorological data measured and recorded by
71 the weather station of Dar El Beida (Algiers), mean annual precipitation (P) for the period between
72 2006 and 2016 came to 644 mm (www.meteo.dz). The precipitation is very irregular in time and
73 space, reflecting heavy rainfall (occasionally reaching 202 mm) over a small number of days during
74 the year (Meddi et al., 2017). This represents the main cause of episodic flash floods which appear

75 frequently on the central coast (Boutaghane et al., 2020). The knowledge of flash floods is not well
76 documented and studied in Algeria because of the non-availability of Hydrological data in recent
77 years. Nevertheless, the maximum flows (extreme flood flows) recorded for these events before 2011
78 reached 268, 876 and 1489 m³/s for the Nador, El Harrach and Isser rivers, respectively (Karahacane
79 et al., 2020). During the episodic flash flood, rivers transport unconsolidated soils and reworked
80 anthropogenic materials, which can long-term influence the submarine channels (Orani et al., 2019).
81 Thereafter, most of the sediment discharged in the central coastal sea extends offshore from the mouth
82 of the rivers according to an increasing inshore silt gradient characterized by a succession of fine
83 sand, muddy sand, sandy mud, and pure mud (Bakalem et al., 2009).

84 **2.2. Sampling and sample treatment**

85 The sampling campaign of the sediments cores was carried out in August 2017 onboard the ship
86 "Grine Belkacem". Three sediment cores A, B, and Z were taken from three bays (Bay of Algiers,
87 Bay of Bou-Ismaïl, and Bay of Zemmouri, respectively) to cover areas likely to be affected by human
88 activities, while a fourth sediment core (S) was taken off Djinet beach (Fig. 1), in an uncontaminated
89 area with the trace metals (Ahmed et al., 2018). Details of the sampling stations are given in Suppl.
90 Tab.1. The four sediment cores were sampled using an Uwitec® gravity sediment corer. Cores were
91 sub-sampled at 1 cm thick intervals for the top 10 cm except for the top interval sliced in two 0.5 cm
92 parts, and then the samples were taken every 2 cm until the bottom. The sliced subsamples (n = 87)
93 were sealed separately in polyethylene bags and stored below 0°C. After their transport to the
94 laboratory, the subsamples were weighed before and after freeze-drying to determine the total water
95 (TW) content.

96 **2.2.1. Grain size, sulfur and organic matter analyses**

97 Samples for particle sizing were measured at the Laboratory of Science in Industrial Process
98 Engineering (USTHB) using a laser analyzer Mastersizer 2000 (Malvern PANalytical corporation),
99 which is applicable to the grain size ranging from 0.02-2000 µm. Sediment samples were pretreated

100 with a solution of H₂O₂ (30 %) and distilled water (1:3) and washed to remove salts and organic
101 debris (Romana et al., 2018). Samples were dried at 105° C, gently crushed in an agate mortar, and
102 homogenized by straining through 2-mm nylon sieved. The first stage of analysis was to gradually
103 add a quantity of the sieved sample into a measuring system of the laser analyzer until the obscuration
104 was between 10 and 20%. By circulating the sample in the measuring system using a stirring and
105 sonication device, a detector records the beam diffracted off of the particles in suspension. Each
106 sample was measured under the same conditions: 2800 r min⁻¹ stirring rate, 3 min sonication, and
107 10%-20% obscuration (Liu et al., 2014). All the analysis steps are described in detail by Ryzak and
108 Bieganowski (2011). The particle size distribution in this work was evaluated as a percentage
109 representation of grain-size fractions according to ISO14688 (2002).

110 The determination of total sulfur content (%) was carried out at Nuclear Research Centre (DRARIA)
111 using an elementary analyzer TruSpec Micro CHNS (Leco company) which is equipped with a
112 dynamic flux infrared cell for the detection and quantification of the element as SO₂. According to
113 Gazulla et al. (2012), the samples of fine sediment (0.350 g) are placed in cordierite boats, which
114 were introduced in a ceramic furnace and combusted at 1350 °C in a pure oxygen environment
115 (2.4 bar ± 10 %). During this process, the sulfur-bearing compounds broke down and liberated free
116 sulfur, which was oxidized to form SO₂ (Andrade et al. 2009). The method was validated using
117 certified reference materials STSD-1 from Canadian Certified Reference Material Project with 0.18
118 ± 0.05 % m/m S (Lynch, 1990).

119 The organic matter (OM) content was determined at the Laboratory of Marine and Coastal
120 Ecosystems (ENSSMAL) by measuring the loss on ignition (LOI) of the sample after calcination in
121 a muffle furnace at 550 °C for 4 h following the method described by Heiri et al., (2001).

122 **2.2.2. Chemical element analyses**

123 Trace and major element concentrations in cores A, B, Z and S (including the background samples)
124 were analyzed at CEREGE (Aix-en-provence, France). The freeze-dried sediment samples were

125 crushed to powder within an agate mortar, then a quantity of 100 ± 5 mg of this sample was weighed
126 in Teflon micro-wave tubes, and 3 ml of 70 % HCl, 4 ml of 67 % HNO₃, 1 ml of 35 % H₂O₂ and
127 0.5 ml of 47 % HF (VWR Chemicals, all of trace grade quality) were progressively added into the
128 tubes. The mixtures were digested under high temperature and pressure conditions in a single reaction
129 chamber (SRC) microwave (Milestone UltraWAVE® microwave). A rack of 12 samples is
130 automatically lowered in the reaction chamber, the chamber is sealed and pressurized with an inert
131 gas (N₂, 99.5 Linde, pressure 30 bars), then a five-step digestion procedure is applied, microwave
132 energy is auto-regulated to achieve the temperature criteria (step 1 ramp from RT to 120 °C in 15
133 min, step 2 stay 120 °C during 15 min, step 3 ramp to 220 °C in 15 min, step 4 stay at 220 °C during
134 20 min and the step 5 cooling to RT, pressure release, rack automatically lifted up). After cooling,
135 the residues of the digestion were diluted with 2 % ultrapure HNO₃ to 50 ml PE tubes and stored at
136 4 °C. The digested steps used in the present study was described by Inal et al. (2018) and Benhalima
137 et al. (2022), and recommended by the European Centre for Research and Teaching in Environmental
138 Geosciences (CEREGE). Total concentrations of trace metals (Mn, V, Co, Ni, Cr, Cu, Zn, Pb, As,
139 Ag, and Cd) and major elements (Fe, Al and Na) were measured in CEREGE (France) using
140 inductively coupled plasma mass spectrometry (ICP-MS, PerkinElmer NexION 300X, USA) and
141 inductively coupled plasma atomic emission spectrometry (ICP-AES, PerkinElmer Optima 4300 DV,
142 USA), respectively.

143 **2.2.3. Quality assurance and quality control**

144 All dilution and preparation of solutions was carried out with Ultrapure water (resistivity N18 MΩ
145 class) obtained from Milli-Q Element system (Millipore, USA). All of the vessels, PE and teflon were
146 soaked in 10 % HNO₃ for at least 24 h and then carefully rinsed with MilliQ water. The calibration
147 curves were established using multi-solution standards CCS4, CCS5, and CCS6 from inorganic
148 ventures (New Jersey, USA) diluted in 2 % HNO₃ solution. The internal standards for ICP-MS and
149 ICP-AES were Rh-103 and Y, respectively. Three replicates of each sample were analyzed to control

150 the precision of measurements, and the results showed that the relative deviations were generally
151 below 5 %, except for cadmium was 2-40 %. All analytical results were presented with their expanded
152 uncertainties (Suppl. Tab. 5): $Ue = k uc$ where uc is the combined standard uncertainty and k is a
153 coverage factor ($k = 2$) as reported in Rasul et al. (2018). The accuracy and precision of ICP-MS and
154 ICP-AES analyses and the possible loss of elements during the digestion steps were checked by the
155 use of Certified Reference Materials CRM020-050, CRM008-050, and CRM 7200 (Suppl. Tab. 2).
156 In all cases, replicate sediment samples were analyzed along with replicates of these reference
157 materials and appropriate blanks at the CEREGE labs (France).

158 **2.3. Risk assessment methods of trace metals contamination**

159 The geologic substrate is generally the main natural source of inorganic chemical species in the
160 ecosystem. However, anthropogenic activities may introduce high amounts of these elements into the
161 coastal zone, making it now sometimes difficult to differentiate natural from anthropogenic
162 components (Belhadj et al., 2017). The common approach used to estimate the anthropogenic impact
163 on sediment chemistry is to compare the metal content of a sediment sample with shale, upper
164 continental crust, and fine-grained sediment (Guo and Yang, 2016). Viers et al. (2009) suggested that
165 the chemical composition of such reference materials used for normalization does not necessarily
166 represent the local geological substratum. For the contamination assessment, considering the
167 mineralogical and physicochemical characteristics of the study area that may imply natural
168 enrichment or depletion for some chemical elements, the use of background levels measured in
169 uncontaminated sediments of the same sampling area was preferred instead of the average crustal
170 composition (Abraham and Parker, 2008). Numerous studies have used the deep unpolluted levels of
171 the cores to represent the natural geochemical composition of sediments (Guo and Yang, 2016;
172 Morelli et al., 2012; Orani et al., 2019; Romano et al., 2018). Therefore, the average concentrations
173 of metals in the deepest three samples of core S are taken as local background values for the
174 calculation of different pollution assessment indices. The use of core S as background is justified by

175 the low trace metal concentrations and a very constant trend of almost all elements' profiles along the
176 depth, as shown in supplementary data (Fig. 1S and Tab. 5S).

177 **2.3.1. Enrichment factor (EF)**

178 A very common approach to estimating the anthropogenic impacts on coastal sediment is to calculate
179 a normalized enrichment factor (EF) for metal concentrations above unpolluted sediment levels (Ip
180 et al., 2007; Kouidri et al., 2016). Chester and Stoner (1973) developed the enrichment factor formula,
181 which has been used by many authors (Ahmed et al., 2018; Benhalima et al., 2022; Bing et al., 2016;
182 X. Gao et al., 2015; Guendouzi et al., 2021; Lin et al., 2016; Zhu et al., 2017). The enrichment factor
183 (EF) was calculated for each sub-sample of the sediment core using the following equation:

$$184 \quad EF = (Element/Fe)_{Sample}/(Element/Fe)_{Background} \quad (\text{Eq. 1})$$

185 Where $(Element/Fe)_{Sample}$ is the ratio of the element concentration in a given sample to Fe, while
186 $(Element/Fe)_{Background}$ is the natural background value of the ratio among the same elements and Fe.
187 Al or Fe are often been used as reference metals (Bachouche et al., 2017) to determine whether the
188 sediment sample was enriched with metals when compared to the natural conditions. Other metals
189 have been proposed for the calculation of EF such as Ca, Ti, Sc and Mn (Salmanighabeshi et al.,
190 2015). In this assessment, iron was taken into account in the EF calculations, the choice of Fe as a
191 reference metal (Eq. 1) will be discussed further later in section 3.4.1.

192 **2.3.2. Pollution load index (PLI)**

193 Another commonly used approach in sediment analysis is the Pollution Load Index (PLI) proposed
194 by Tomlinson et al. (1980) to assess the sediment quality and the degree of trace metal pollution in
195 aquatic ecosystems. It is defined as the n^{th} root of the product of n contamination factors (CF):

$$196 \quad PLI_{site} = \sqrt[n]{(CF_1 \times CF_2 \times CF_3 \times \dots \times CF_n)} \quad (\text{Eq. 2})$$

197 Where, CF: contamination factor; and n: number of metals examined.

198 **2.4. Sediment quality guidelines**

199 Numerous sediment quality guidelines (SQGs) have been developed in North America to measure
200 adverse biological effects on aquatic organisms upon exposure to sediment-bound contaminants
201 (Long and MacDonald, 1998). Two sets of SQGs were developed for freshwater and marine
202 ecosystems as non-regulatory benchmarks to facilitate interpretation of chemical data, effect range
203 low/effect range median values (ERL/ERM), and the threshold effect level/probable effect level
204 (TEL/PEL) (Bakan and Özkoç, 2007). ERLs and TELs refer to the concentrations below which
205 harmful effects upon sediment-dwelling fauna would only rarely be expected. In contrast, ERMs and
206 PELs indicate concentrations above which adverse biological effects would always be observed
207 (Long and MacDonald, 1998). However, the concentrations that fall between the ERLs/TELs and
208 ERMs/PELs correspond to a range in which effects on live sediment organisms occasionally occur.
209 Mean sediment quality guideline quotients (Qm-SQG) have been proposed by Long et al. (2006) to
210 estimate the toxicological risks of contaminant mixtures in sediment samples. In this study, mean
211 SQG quotients were determined by dividing the concentrations of metal by their respective SQGs
212 values such as the effects range low (ERM) and probable effect level (PEL), and averaging the
213 obtained quotients for individual chemicals. Qm-SQG can be expressed as:

$$214 \quad Qm - SQG = \sum_{i=1}^n (Mi/SQGi)/n \quad (\text{Eq. 3})$$

215 Where M_i is the concentration of the i^{th} metal, $SQGi$ is the guideline corresponding to ERL or TEL
216 values for the metal, and n is the number of metals. The probabilities of toxicity in marine sediments
217 increase as chemical concentrations of heavy metals increase relative to empirically derived sediment
218 quality guidelines. According to Long et al. (2000), Sediment with Qm-ERM values less than 0.1,
219 0.11-0.5, 0.51-1.5, and > 1.50 are predicted to be toxic by 9 %, 21 %, 49 %, and 76 % to sediment-
220 dwelling organisms, respectively, while for Qm-PEL, the values of < 0.1 , 0.11-1.5, 1.51-2.3 and > 2.3
221 corresponds to 8 %, 21 %, 49 % and 73 % likelihood of toxicity in sediments, respectively.

222 **2.5. Statistical analyses of data**

223 Pearson correlation analysis was conducted for each core to establish geochemical associations and
224 behavior of the elements in sediments. A two-tailed Pearson's coefficient was used in correlation
225 analysis. Principal component analysis (PCA) was performed to check the factors that control the
226 geochemical origin of the elements in coastal sediments. PCA was subjected to varimax rotation with
227 the Kaiser normalization method to maximize each factor's component loadings and eliminate invalid
228 components. All variables were tested by Kaiser-Meyer-Olkin and Bartlett tests. Statistical
229 processing of the data was performed using SPSS software 22.0.

230 **3. Results and Discussion**

231 **3.1. Variation of sediment properties**

232 The sediment properties, such as organic matter “OM”, total water content “TW”, total sulfur “TS”,
233 and grain size, are key factors affecting the behavior and mobility of metals in marine sediments. The
234 vertical distributions and full data of OM, TW and TS in cores A, B and Z are shown in Fig. 2 and
235 Suppl. Tab. 3, respectively. OM contents were significantly higher in core A located in Algiers Bay,
236 than in the other cores. The contents increased rapidly from the bottom of the core to about 9 cm of
237 depth and presented a wide variability ranging from 9.1 % to 13.3 %. The primary source of OM
238 inputs in Algiers Bay is believed to derive from the allochthonous C fluxes, like domestic and urban
239 effluent in El Harrach river, and represent a severe effect that impacts the ecosystems and sediment-
240 dwelling organism's health (Bakalem et al., 2009; Benhalima et al., 2022; Boudjema et al., 2014). In
241 contrast, significant increases in the top of the cores B and Z (up to 11.7 % and 10.8 %, respectively)
242 were found, suggesting rapid burial of freshly deposited organic carbon following massive inputs
243 from urban and agricultural wastewater discharges. This leads to rapid remineralization of OM near
244 the oxic-suboxic interface (Kristensen et al., 2008). Compared with the evident increasing trend
245 towards the topmost interval of cores B and Z, the OM content in core A exhibited a marked decrease

246 above 9 cm of depth due to the diversion of El Harrach effluents to the Baraki wastewater treatment
247 plant in 2007 and following the increase in the treatment capacity of the station in 2015. The partially
248 treated effluents discharged from the wastewater plant to El Harrach river have a beneficial effect in
249 total sulfur content which decreased in the topmost interval of core A from 0.9 to 0.25 % (Fig. 2,
250 Suppl. Tab. 3). On the other hand, the TS content was markedly decreased from the bottom until the
251 4 cm depth in core B, whereas it remained fairly stable along the core Z except for the moderately
252 high peaks observed at 2, 14 and 16 cm of depth (Fig. 2). The high TS contents in cores B and Z
253 probably traduce enrichment by diagenetic processes resulting from the biological sulfate reduction
254 in these depths (Appelo and Postma, 2004).

255 The cores sampled from the three bays of the central Algerian coast consist of three sediment types
256 (silt, clay, and traces of fine sand). The basic statistics on textural data and mean grain size are listed
257 in Suppl. Tab. 4. Observations reveal that the three fractions vary in the study area. On the whole, the
258 sediments are dominated by silt, which accounts for more than 67 %. This is followed by clay, with
259 an average mass percentage of 20.8 %, while fine sand, is the smallest fraction in sediment with a
260 mean percentage of 2.63 %. These findings indicate that the high supply of fine sediments in the study
261 area was probably due to the lack of substantial river inputs (Ergin and Yörük, 1990) and the increased
262 episodic floods and associated mudflows during the last decades (Taieb Errahmani et al., 2020). The
263 results of texture analysis additionally show that the average grain size followed the order of core A >
264 core B > core Z, ranging from 10.5 μm for core A to 6.75 μm for core Z with a mean value of 9.24 μm
265 (Suppl. Tab. 4), suggesting a relatively stable sedimentary environment at all the sites (Liu et al.,
266 2011). Overall, for all cores percentages of OM, TW, TS and Silt ranged [8.6 - 13.3] %, [32.23 -
267 50.86] %, [0.15 - 0.9] % and [67.57 - 82.11] %, respectively, and decreased in the following order:
268 core A > core B > core Z. These findings indicate that the central Algerian coast sediments are
269 waterlogged and very fine, rich in total sulfur and organic matter favoring further the accumulation
270 of trace metals, especially in Algiers Bay, which displayed the highest values for sediment properties.

271 **3.2. Trends of major and trace element concentrations in core samples**

272 A statistical summary of chemical analyses on major and trace elements is presented in Table 1 (the
273 complete data are reported as supplementary material) and a graphical representation of elements'
274 depth profiles in the three sediment cores A, B and Z is presented in Fig. 3.

275 In core A (Algiers Bay), vertical distributions of Fe, Mn, V, Co, Ni, and Pb showed similar patterns
276 and decreased slightly from the bottom to the surface sediment. Conversely, the concentrations of Cd
277 and Zn exhibited somewhat increasing trends up through the layers with obvious fluctuations in the
278 upper section of the core. For Ag, the depth distribution showed overall increasing contents until 8 cm
279 but decreased in the upper Layers. Meanwhile, As and Na contents showed upward trends in the
280 upper 18 cm. Lastly, Cr followed a similar tendency to Cu, and the maximum concentrations of both
281 elements were detected at 12 cm of depth. At this site, the average concentrations Zn, Cu, Cd, Pb,
282 and Ag (162 ± 2.67 , 34.8 ± 0.97 , 0.29 ± 0.03 , 44.4 ± 1.27 and 0.71 ± 0.01 mg.kg⁻¹, respectively) are
283 significantly higher than those for the other sites and exceed the background values (Tab. 1). In fact,
284 the samples collected in Algiers Bay suggest a significant role of Algiers' urban and industrial sites
285 (Chemrouk and Chabbi, 2016). In particular, Zn, Cd, and Ag reach contents in the topmost sediments
286 as high as 180, 0.39, and 0.87 mg.kg⁻¹, respectively. The elevated concentrations of metal are also
287 explained by a high input of anthropogenic contaminants from the port of Algiers (Bachouche et al.,
288 2017) and likely from the direct discharge of greywater from ships in the sea area (Ytreberg et al.,
289 2020).

290 In core B (Bou Ismail Bay), concentrations of Fe, Al, V, Co, Ni, Cr, Cu, Zn, Cd, Ag, and Pb uniformly
291 decreased from the bottom to the top of the core and the maximum concentrations of these elements
292 were observed at the bottom sediment layers (Fig. 3). The high loads of these elements were probably
293 caused by the increase in total sulfur contents in the bottom sediments (Fig. 2, 3). This suggests the
294 precipitation of metal sulfide under anoxic conditions (Komada et al., 2016). In contrast, Mn, As, and
295 Na increased significantly and reached the maximum in recently deposited sediments. The presence

296 of the Mn peak value (315 mg.kg^{-1}) at the top of the core in correspondence with the high organic
297 matter content (Fig. 2, 3, Suppl. Tab. 3) could be due to an upward movement of secondary oxidants
298 under the influence of the early diagenesis process. However, this point cannot be confirmed here
299 because of the lack of the analyses of the oxidation-reduction index in the pore water of sediments.

300 In core Z (Zemmouri Bay), the depth profiles of Fe, Mn, Co, Cu, Zn, Ag, and Pb showed similar
301 trends, and the concentrations were all lower at the bottom section of the core and higher at the
302 surface. The minimum concentrations of these elements were observed at 9 cm of depth except for
303 Ag and Pb and then demonstrated an increasing trend toward the top. As and Na showed increasing
304 trends from the bottom, while Cd, V, Cr and Ni did not follow an increasing tendency and remain
305 relatively stable. In detail, the concentrations of Fe and Mn showed high variability with depth, and
306 increased distinctly upwards from 9 cm of depth ranging from 30 to 43 g.kg^{-1} and 191 to 314 mg.kg^{-1} ,
307 respectively. These high levels in the top layers are due either to the changes in the terrigenous
308 inputs (Orani et al., 2019), or represent a surface diagenetic enrichment (Janaki-Raman et al., 2007).
309 Moreover, some trace metals such as Co, Cu, Zn, Ag, Pb, and As showed increasing concentrations
310 in surface layers (up to 13.1, 24.3, 130, 0.31, 32.6 and 18.5 mg.kg^{-1} , respectively), suggesting
311 increasing metal loads probably from anthropogenic origin unless the distribution of such metals are
312 affected by post-depositional diagenetic processes. However, the average concentrations of most
313 elements are close to the natural background values (Table 1) and relatively low with respect to those
314 found in Algiers Bay sediments where the influence of anthropogenic activities can be easily
315 recognized.

316 Overall, all cores A, B, and Z showed maximum arsenic concentrations (up to 20.1, 21, and 18 mg.kg^{-1}
317 respectively) in upper sediments (Table 1, Figure 3), which is in good agreement with the results
318 obtained by Inal et al. (2018) for arsenic (21.3 mg.kg^{-1}) in surface sediments of the central Algerian
319 coast. Since arsenic serves usually as a marker of agricultural runoff (Bai et al., 2012; Sun et al.,
320 2012), the increasing trends of arsenic toward the top layers of the three sediment cores (Fig. 3)

321 indicate the increasing use of arsenic compounds as fertilizer, manure, and agrochemicals in
322 agricultural fields (Mao et al., 2020). The results additionally show that the Fe was the most abundant
323 element in all the cores, with concentrations ranging from 29.9 to 45.7 g.kg⁻¹ and were far higher than
324 the Al concentrations, which varied between 3.6 and 21.9 g.kg⁻¹. This abundance is a result of an
325 additional supply of iron-rich secondary phases from the aeolian dust of the Algerian Sahara (Hassani
326 et al., 2019) in addition to the terrigenous source in semi-arid environments with low runoff (Viers et
327 al., 2009). The elevated level of Fe in such an environment can highly influence trace metal levels in
328 coastal sediment (Janaki-Raman et al., 2007). Therefore, the depth profiles of most trace metals in
329 the study area showed similar patterns to Fe (Fig. 3) due probably to the low-level inputs that
330 characterize the Algerian rivers.

331 **3.3. Geochemical behavior and sources of trace metals**

332 **3.3.1. Correlation analysis**

333 In order to strengthen the interpretation of the results and highlight the common patterns and
334 geochemical behavior of the elements, a Pearson's correlation test was performed for each sediment
335 core (Tab. 2). The grain size distribution of sediment particles was not included in this analysis since
336 fine silty clays are dominant in all the cores. In core A, some trace metals like Pb, V, Co, Ni, Cr, and
337 Cu present significant positive correlations ($p < 0.01$) to one another and to Fe, Mn, and Al (except
338 Co with Al), indicating that they were bound to Fe, Mn, and Al oxyhydroxides. As already mentioned,
339 Zn and Cd had similar distributions along the core A, and Pearson's correlation confirms a high
340 relationship between both elements ($p < 0.01$; $r^2 = 0.72$). Additionally, Ag was positively correlated
341 with Zn and Cd ($p < 0.05$; $r^2 = 0.47$), but no positive correlations were obtained for Ag with the major
342 elements or other trace elements, which indicates the anthropogenic source of Ag and a different
343 origin from the other metals. The relationship between organic matter contents and chemical elements
344 was analyzed by Pearson's correlation (Tab. 2); thus, positive correlations are observed between OM
345 and Zn, Cd, and Ag metals ($0.55 < r^2 < 0.66$), which suggests that organic matter acted as a sink or

346 source for these metals in sediment (Komada et al., 2016; Martínez-Santos et al., 2015). Finally, Na
347 and As were significantly correlated with each other ($p < 0.01$; $r^2 = 0.79$) and with TW ($p < 0.01$)
348 suggesting mobility of both elements in the sediments. However, Arsenic showed no positive
349 correlation with the other elements, indicating that the anthropogenic signal of As were relatively
350 high in Algiers Bay.

351 In core B, trace metals like Pb, V, Cr, Co, Ni, Cu, Zn, Cd, and Ag showed very significant correlations
352 with Fe ($0.63 < r^2 < 0.97$; $p < 0.01$) and to a lesser extent with Al (Tab. 2), implying that they were
353 more adsorbed by Fe oxyhydroxides than Al. Furthermore, the concentrations of these trace metals
354 (as well as those of Fe and Al) showed an excess when compared to the high TS content and low OM
355 in deep layers of core B (Fig. 2, 3). These findings indicate the precipitation of metalliferous sulfide
356 (Fu and Wang, 2011) following SO_4^{2-} reduction and the formation of H_2S under an anoxic reduced
357 environment (Hong et al., 2020). On the other hand, Mn was positively correlated to OM and TW
358 ($p < 0.01$). Apparently, the early diagenetic process played a major role in the vertical distribution of
359 Mn indicating a peak in the upper layer. The high Mn values at the surface level are attributed to the
360 supply of dissolved Mn^{2+} from the reduced sediment layer which oxidized to Mn^{4+} at the surface
361 (Pattan et al., 2019). As and Na additionally exhibited strong positive correlations to Mn, OM, and
362 TW ($p < 0.01$) and also a significant positive correlation with each other ($r^2 = 0.84$). The increase in
363 As contents in surface sediment of the core suggests the presence of recent anthropogenic input of
364 this element under reducing conditions and its sorption onto the newly formed Mn oxyhydroxides in
365 the sedimentary water column (Ontiveros-Cuadras et al., 2021).

366 In core Z, Pearson correlation coefficients computed for Fe and Mn showed close relationships to Na,
367 Pb, V, Cr, Co, Ni, Cu, Zn, and As; meanwhile, Al exhibited positive correlations only with Cr and V.
368 The correlation analysis also displayed positive correlations between Fe and OM or Mn and OM
369 ($p < 0.01$) indicating diagenetic modifications and resuspension processes for both elements. In fact,
370 the increased carbon flux can change the redox conditions in sediments overlain by the oxygenated

371 bottom waters (Pattan et al., 2019) thereby increased the solubility for redox-sensitive metals like Fe
372 and Mn (Charriau et al., 2011). The obtained positive correlations between (Fe-TW), (Mn-TW), and
373 (OM-TW) may support the efficiency of this mechanism (Tab. 2). Similarly, some trace metals such
374 as Pb, Co, and Zn were correlated positively to OM and TW, and significantly to Fe and Mn (Tab.
375 2), which explains probably their increasing concentrations in the oxic conditions (upper sediment
376 layers) compared to suboxic conditions (Fig. 3). This suggests the remobilization of Pb, Co, and Zn
377 through metal scavenging (Ontiveros-Cuadras et al., 2021). However, no significant correlation was
378 obtained for Cd with major elements, and it only showed positive correlations with V and Cr
379 ($p < 0.01$), indicating that Cd, V, and Cr depositions were affected by the same process in the
380 sediments. Lastly, no statistically significant correlation existed between TS and most elements,
381 which was possibly due to the dissolution of various metals sulfides (Morse and Luther, 1999).

382 From the simple observation of Pearson correlation results and element variation along the cores, it
383 appears that the vertical distribution of trace metals in cores B and Z has been modified to some extent
384 by diagenetic processes. It is equally clear that core A showed significant changes in some of the
385 analyte concentrations with different metal inputs, most probably of anthropogenic origin given the
386 location of the sampling station.

387 **3.3.2. Principal component analysis (PCA)**

388 To further examine the origin of the elements in the study area, a Principal Component Analysis
389 (PCA) was performed for each sediment core (Tab. 3, Suppl. Fig. 2). PCA has been applied
390 successfully from a correlation matrix including 17 variables (OM %, TS %, TW %, Fe, Mn, Al, Na,
391 V, Cr, Co, Ni, Cu, Zn, Pb, As, Ag, and Cd). The variables used all passed the Kaiser-Meyer-Olkin
392 (KMO > 0.62) and Bartlett ($p < 0.001$) tests, confirming the suitability of the dataset for PCA.

393 Four principal components (PC) with eigenvalues higher than one were extracted from the variables
394 in sediment core A, which accounted for 88.65 % of the total variance (Tab. 3). The first two

395 components accounted for 68.82 % of the total variance and reflected the most important information,
396 with PC1 (45.96 % of the variance) characterized by strong loading on Fe, Mn, Pb, V, Cr, Co, Ni, Cu
397 (from 0.72 to 0.98), and PC2 (22.86 %) mainly characterized by high positive loadings of variables
398 such as OM, Zn, Cd, and Ag (from 0.74 to 0.88). PC1, therefore, represents the natural source of
399 sediments such as the weathering of parent rock materials, and PC2 represents the elements (Zn, Cd,
400 and Ag) retained in organic material and, consequently, described the anthropogenic source of
401 sediments. Given that OM origin in Algiers bay sediments was primarily related to direct inputs from
402 El Harrach river (Bakalem et al., 2009), we infer that the major sources of Cd, Zn and Ag in core A
403 were the municipal effluents and surface runoff. PC2 could also be derived from agricultural activities
404 because phosphorus fertilizer has been generally regarded as the main source of Cd and Zn in
405 agricultural areas (Jiao et al., 2015). The third component (PC3) accounted for 14,11 % of the total
406 variance and had strong loading values on As, Na, and TW (PCA coefficients > 0,89) suggesting that
407 PC3 presents the mobile fraction of sediment. Lastly, the fourth component (PC4) accounted for
408 5.72 % of the total variance and had high loading on TS (0.85). The detected high TS content in core
409 A (Fig. 2) seems to be the consequence of the direct inputs from El Harrach river into Algiers Bay.
410 For the sediment core B, the dataset used for PCA analyses gave two major components with
411 eigenvalues > 1 and explained 86.43 % of the total variance (Tab. 3). The first component extracted
412 (PC1) explained the most variance (72.29 %) and had high positive loading on Fe, Al, Pb, V, Cr, Co,
413 Ni, Cu, Zn, Cd and Ag. Since Fe and Al are generally derived from weathering and erosion of rocks
414 and soil parent materials (Li and Li, 2017), PC1 was considered the lithogenic source of metals bound
415 in oxihydroxide minerals. Furthermore, PC1 is characterized by the strong association of almost all
416 analytes (except Mn, Na, As) with TS (reducible and/or oxidisable fractions of S), which indicates
417 that they were mainly associated with sulfide fraction. The second component (PC2) accounted for
418 14.14 % of the total variance and included Mn, Na, As, OM and TW with high loading (from 0.75 to
419 0.96). Here, the strong positive effect of OM and TW with the Mn suggests that the latter had great

420 mobility and clearly indicated early diagenetic events in sediments. In light of the results of Pearson
421 correlations and PCA, PC2 is considered to be both the mobile fraction of the sediment and the
422 anthropogenic contaminant associated with the discharge of urban and agricultural wastewater.

423 PCA performed on core Z gave four significant PCs with eigenvalues > 1 , explaining 91.65 % of the
424 total variance (Tab. 3). The principal components PC1, PC2, PC3 and PC4 accounted for 54.21 %,
425 22.86 %, 10.43 % and 4.15 % of the total variance, respectively. PC1 (54.21 %) is the most important
426 component and was mainly characterized by high positive loadings of variables such as Fe, Mn, Pb,
427 V, Cr, Co, Ni, Cu, and Zn. This indicates that PC1 described the lithogenic source of elements that
428 were principally retained in the crystal lattices of secondary minerals and, consequently, had low
429 mobility (Martínez-Santos et al., 2015). Moreover, some of these variables (Fe, Mn, Pb, Co, and Zn)
430 also had moderate to high positive loadings in PC2, suggesting the partial dissolution and mobility of
431 these elements in the sedimentary water column due to a marked increase of OM content in surficial
432 sediments (Fig. 3) which acts as an electron donor, thus, reducing Fe or Mn oxyhydroxides (Moushmi
433 et al., 2022). This is very well supported by the strong loadings of TW and OM (0.98 and 0.72,
434 respectively) in PC2. A close observation of Tab. 3 results shows that Ag and As had high loadings
435 only on PC2 suggesting they were potentially mobile and bioavailable in sediment. In light of the
436 result of PCA, we infer that PC2 is regarded as an anthropogenic source of OM, As and Ag mainly
437 related to direct input from agricultural wastewater and untreated urban sewage. The third principal
438 component (PC3) consists only of Al, V, Cr and Cd (From 0.64 to 0.78), suggesting that PC3
439 described the lithogenic source bound in aluminosilicate minerals (Guo and Yang, 2016). However,
440 according to the Pearson correlation analysis, Cd did not show a positive correlation with Al. These
441 results may indicate the anthropogenic origin of Cd in sediments of Zemmouri Bay. With regard to
442 PC4, TS was the only variable with significant positive loading (0.98), indicating that sulfates did not
443 influence the trace metal contents, as was previously stated.

444 **3.4. Assessment of Anthropogenic impact**

445 **3.4.1. Enrichment factor (EF)**

446 Like in many developing countries, the Algerian coast suffers deterioration as a result of demographic
447 pressure and untreated discharges from human activities (Abderrahmani et al., 2021; Inal et al., 2018;
448 Guendouzi et al., 2020). According to Chen et al. (2007), EFs with very low values ($EF < 1$) indicate
449 negligible or none enrichment, $EF < 2$ represent slight enrichment, 2-5 account moderate enrichment,
450 5-10 implies moderately severe enrichment, 10-25 shows severe enrichment, 25-50 display very
451 severe enrichment and finally, $EF > 50$ suggests extremely high enrichment. However, the assessment
452 of trace metal concentrations in the sediment was difficult to interpret because there is no single
453 reference element that exists for normalization. For this purpose, we used Fe as a reference metal to
454 calculate EFs because of the predominance in the study area of Fe-rich secondary phases exclusively
455 of geogenic and eolian origin. Furthermore, it is noteworthy that many authors have used Fe
456 successfully for geochemical normalization (Ahmed et al., 2018; Bachouche et al., 2017; Moushmi
457 et al., 2022; Ranjan et al., 2018).

458 According to the local background values determined in this work, the results of the EF's mean and
459 surface values are shown in Fig. 4 and Suppl. Tab. 6, from which it can be found that the enrichment
460 degree of trace metals varies within a narrow range (from 0.95 to 3.36) in all sediment cores. In other
461 words, the EFs for the sediment samples were all classified as deficient or no enrichment to moderate
462 anthropogenic enrichment. The contamination order of these metals in the whole of the study area
463 was $Cd > Ag > Pb > As > Zn > Cu > Ni > Cr > V > Co$ (Fig. 4). In detail, almost all EF values of Ni,
464 Cr, V, and Co on the central coast were very close to or less than 1 demonstrating a crustal origin of
465 these metals in the study area (Suppl. Tab. 6). While the EF values of Zn, Cu, Cd, Pb, As, and Ag
466 were greater than 1 as a whole, and some of them were over 2 or even 3 in surface sediments of core
467 A, indicating moderate contamination by these trace metals in Algiers Bay. The high EF values at
468 sediments of core A can be attributed to direct discharges of contaminants from industrial activities,
469 refineries and oil factories in the inner part of the Algiers port and El Harrach river, which also carries

470 a significant part of pollution in Algiers Bay (Bachouche et al., 2017). On the other hand, the results
471 showed that some of the EF values of trace metals in surface sediment were higher than in average
472 sediment in cores A and Z, which indicated that anthropogenic trace metals have been recently
473 deposited in sediments during the increasing urbanization in recent years. The EF values of trace
474 metals were plotted against depth profiles, and increasing trends of As EFs profiles were detected in
475 all sediment cores (Suppl. Fig. 3). The profiles of EF were similar to the trends in concentrations of
476 Arsenic (Fig. 3), which reflected the agricultural intensification over the two past decades. For some
477 trace metals, slight to moderate EF values occurred only in some layers of the cores, indicating
478 anthropogenic enrichments of these elements for a certain period.

479 **3.4.2. Pollution load index (PLI)**

480 The PLI introduced by Tomlinson et al. (1980) has been used in the present study to evaluate the
481 sediment's environmental quality and compare the overall metal load in sediments at each site (Fig.
482 5). Two classes of the PLI value have been identified: When $PLI < 1$, it means there was no pollution
483 of coastal sediments; otherwise $PLI > 1$, sediments are moderate to highly polluted. Thus, as metal
484 pollution increases in sediment, the PLI value also increases. The results show that PLI values in deep
485 sediments are lower than at the surface in cores A and Z, indicating recent contamination of some
486 trace metals in Algiers and Zemmouri Bays. The calculated PLI values for all cores followed the
487 decreasing order core A > core B > core Z. The highest PLI value was calculated for core A,
488 indicating that Algiers Bay was moderately polluted by metals where sediment quality might be
489 deteriorated by trace metals especially As, Cd, Pb, Zn, Cu and Ag. Indeed, the Bay of Algiers was
490 previously classified as a hot spot priority in the Mediterranean Sea (UNEP/WHO, 1999). However,
491 the load indices calculated for Bou Ismail and Zemmouri Bays revealed that the metal pollution was
492 relatively low compared to Algiers Bay which showed moderate enrichment for some trace metals
493 mentioned above.

494 **3.5. Application of sediment quality guidelines**

495 The ecological risk of trace metals in the aquatic sediment was evaluated by comparing the
496 concentrations present at the surface of the cores with the respective SQGs (Suppl. Fig. 4). Cd and
497 Ag concentrations were below the TEL values (0.68 mg.kg^{-1} and 0.73 mg.kg^{-1} , respectively) and ERL
498 values (1.2 mg.kg^{-1} and 1 mg.kg^{-1} , respectively) in all the sediments core, while Zn concentrations
499 were below the TEL value (124 mg.kg^{-1}) and ERL value (150 mg.kg^{-1}) only in cores B and Z.
500 Moreover, the concentrations of Cu in cores B and Z were also lower than the ERM value (34 mg.kg^{-1})
501 but exhibited higher values than TEL (18.7 mg.kg^{-1}). The results also showed that Pb contents in
502 cores A and B exceeded the TEL value of 30.2 mg.kg^{-1} . However, none of the sites exceeded the ERL
503 value (46.7 mg.kg^{-1}). These findings imply that organisms living within or near sediments are rarely
504 exposed to adverse biological effects. For As, Ni and Cr in the three cores, Zn and Cu in core A, all
505 the concentrations ranged between their respective ERMs and PELs, indicating that biota might be
506 occasionally exposed to toxic effects.

507 For the toxicity evaluation of combined trace metals, Qm-SQGs calculated based on Ni, Cr, Cu, Zn,
508 Pb, As, Cd and Ag ranged in all cores from 0.21 to 0.26 for m-ERM-Q, and 0.34 to 0.43 for m-PEL-
509 Q (Fig. 5), which coincide with a 21 % probability of being toxic for living species according to the
510 toxicity probabilities of m-ERM and m-PEL quotients (Long et al., 2000). The average Qm-SQG
511 values of the sediment cores ranked as follows: Core A > Core B > Core Z with slightly higher values
512 in the surface sediments of Algiers (Core A) and Zemmouri (Core Z) bays. Although Ni
513 concentrations in the three cores are within the range of natural variability and cannot be related to
514 human impact according to EF values, this metal contributed significantly (more than 30 %) to Qm-
515 SQG in all cores. These results are consistent with those found by Inal et al. (2018) in surface
516 sediments of the central coast, therefore, the authors suggested more monitoring of Ni inputs in the
517 coastal zone as their ecotoxicological levels are doubtful. However, the contents of As fairly exceed
518 its PEL or ERL values (Fig. 4S), which indicate that As presents a higher ecological risk than the
519 other metals for the aquatic species.

520 **4. Conclusion**

521 This study was conducted to determine the effects of natural and anthropogenic processes on
522 depositional trends and risk of trace metals. The results showed that iron was the most abundant
523 element in the study area (up to 45.7 g/kg) because of the predominance of Fe-rich secondary phases
524 of terrestrial and eolian origin. Most trace metals in the three cores showed similar patterns to Fe, and
525 some of them have been modified to some extent by diagenetic processes, which controlled their
526 distribution in sediments. The local geochemical background was established from the
527 uncontaminated section of the core S located offshore of Cap Djinet and is considered to represent
528 the natural geochemical sediment composition of the central Algerian coast. Thus, the average
529 contents of Zn, Cu, Cd, Pb, and Ag (162 ± 2.67 , 34.8 ± 0.97 , 0.29 ± 0.03 , 44.4 ± 1.27 and
530 0.71 ± 0.01 mg.kg⁻¹, respectively) exceeded their respective natural background values in the Algiers
531 Bay sediments due to the influence of polluted inputs of El Harrach river and the Algiers port.
532 According to Pearson correlation and PCA analyses, rock weathering acted as the major factor
533 contributing to most trace metal accumulation in all cores, whereas As was bound predominantly in
534 the potentially most mobile fractions of sediment and originated mainly from fertilizer application in
535 the region. The influence of organic matter, total sulfur, and total water content on metals behavior
536 were discussed, and the trace metal availability showed different patterns in the three cores:
537 preferential adsorption of Cd, Zn and Ag to the organic matter in core A; precipitation of Pb, Co, V,
538 Ni, Cr, Zn, Cu, Cd and Ag as metalliferous sulfides in core B and diagenetic enrichment of Pb, Zn
539 and Co in core Z. The enrichment factors (EF) decreased in the order Cd > Ag > Pb > As > Zn > Cu >
540 Ni > Cr > V > Co and showed no significant enrichment and pollution in the entire study area.
541 Regarding to SQGs, all metals had no frequent adverse effects on sediment-living organisms. PLI
542 and Qm-SQG values showed that Algiers Bay was the most polluted area and presented a higher
543 ecological risk than the other sites. This information could be useful for the formation of coastal zone
544 management strategies for the marine environment. The improvement of water and coastal sediment

545 quality requires the control of agrochemical application in farmland and the implementation of
546 wastewater treatment plants on the river banks.

547 **Acknowledgments**

548 This research work was financially supported by the French program METMAR-MERMEX as part
549 of the PHC TASSILI project (Code PHC: 17MDU986; Title: Inputs, accumulations and trace metal
550 contaminations in Algiers and Marseille coastal areas) and the directorate-general for scientific
551 research and technological development (DGRSDT). The authors are very grateful to CNRDPA,
552 especially to our colleague Inal Ahmed for their help to carry out the sampling campaign onboard the
553 vessel GRINE BELKACEM, as well as to Djamel Taib Errahmani from CNRA for providing us the
554 sediment corer and for technical assistance during the sampling campaign. The authors are also
555 grateful to our dear colleague Nouredine Djerrai who helped us with the preparation of the sampling
556 map.

References

- 557 Abderrahmani, K., Boulahdid, M., Bendou, N., Guenachi, B., Hacene, O.R., Masino, F.,
558 Montevecchi, G., 2021. Partitioning of trace elements in the tissues of Mediterranean mussels
559 (*Mytilus galloprovincialis*) sampled from industrial sites along the Algerian coast. *Mar. Pollut.*
560 *Bull.* 173. <https://doi.org/10.1016/j.marpolbul.2021.113006>
- 561 Abraham, G.M.S., Parker, R.J., 2008. Assessment of heavy metal enrichment factors and the degree
562 of contamination in marine sediments from Tamaki Estuary, Auckland, New Zealand. *Environ.*
563 *Monit. Assess.* 136, 227–238. <https://doi.org/10.1007/s10661-007-9678-2>
- 564 Ahmed, I., Mostefa, B., Bernard, A., Olivier, R., 2018. Levels and ecological risk assessment of
565 heavy metals in surface sediments of fishing grounds along Algerian coast. *Mar. Pollut. Bull.*
566 136, 322–333. <https://doi.org/10.1016/j.marpolbul.2018.09.029>

- 567 Appelo, C.A.J., Postma, D., 2004. *Geochemistry, groundwater and pollution*, second edition,
568 *Geochemistry, Groundwater and Pollution, Second Edition*. CRC Press.
569 <https://doi.org/10.1201/9781439833544/GEOCHEMISTRY-GROUNDWATER->
570 [POLLUTION-APPELO-DIEKE-POSTMA-APPELO-DIEKE-POSTMA](https://doi.org/10.1201/9781439833544/GEOCHEMISTRY-GROUNDWATER-POLLUTION-APPELO-DIEKE-POSTMA-APPELO-DIEKE-POSTMA)
- 571 Bachouche, S., Houma, F., Gomiero, A., Rabah, B., 2017. Distribution and Environmental Risk
572 Assessment of Heavy Metal in Surface Sediments and Red Mullet (*Mullus barbatus*) from
573 Algiers and BouIsmaïl Bay (Algeria). *Environ. Model. Assess.* 22, 473–490.
574 <https://doi.org/10.1007/s10666-017-9550-x>
- 575 Bai, J., Xiao, R., Zhang, K., Gao, H., 2012. Arsenic and heavy metal pollution in wetland soils from
576 tidal freshwater and salt marshes before and after the flow-sediment regulation regime in the
577 Yellow River Delta, China. *J. Hydrol.* 450–451, 244–253.
578 <https://doi.org/10.1016/j.jhydrol.2012.05.006>
- 579 Bakalem, A., Ruellet, T., Dauvin, J.C., 2009. Benthic indices and ecological quality of shallow
580 Algeria fine sand community. *Ecol. Indic.* 9, 395–408.
581 <https://doi.org/10.1016/j.ecolind.2008.05.008>
- 582 Bakan, G., Özkoç, H.B., 2007. An ecological risk assessment of the impact of heavy metals in
583 surface sediments on biota from the mid-Black Sea coast of Turkey. *Int. J. Environ. Stud.* 64,
584 45–57. <https://doi.org/10.1080/00207230601125069>
- 585 Barbieri, M., Sappa, G., Nigro, A., 2018. Soil pollution: Anthropogenic versus geogenic
586 contributions over large areas of the Lazio region. *J. Geochemical Explor.* 195, 78–86.
587 <https://doi.org/10.1016/j.gexplo.2017.11.014>
- 588 Barron, A., Sun, J., Passaretti, S., Sbarbati, C., Barbieri, M., Colombani, N., Jamieson, J., Bostick,
589 B.C., Zheng, Y., Mastrocicco, M., Petitta, M., Prommer, H., 2022. In situ arsenic

590 immobilisation for coastal aquifers using stimulated iron cycling: Lab-based viability
591 assessment. *Appl. Geochemistry* 136. <https://doi.org/10.1016/j.apgeochem.2021.105155>

592 Belhadj, H., Aubert, D., Dali Youcef, N., 2017. Geochemistry of major and trace elements in
593 sediments of Ghazaouet Bay (western Algeria): An assessment of metal pollution. *Comptes*
594 *Rendus - Geosci.* 349, 412–421. <https://doi.org/10.1016/j.crte.2017.09.013>

595 Benhalima, M., Boulahdid, M., Guendouzi, Y., Radakovitch, O., Aroua, M., Fowler, S.W.,
596 Ambrosi, J.-P., Angeletti, B., 2022. Occurrence, contamination level and ecological risk
597 assessment of dissolved and particulate trace elements in rivers entering the southwestern
598 Mediterranean Sea. *Mar. Pollut. Bull.* 180, 113723.
599 <https://doi.org/10.1016/j.marpolbul.2022.113723>

600 Bing, H., Zhou, J., Wu, Y., Wang, X., Sun, H., Li, R., 2016. Current state , sources , and potential
601 risk of heavy metals in sediments of Three Gorges Reservoir , China *. *Environ. Pollut.* 214,
602 485–496. <https://doi.org/10.1016/j.envpol.2016.04.062>

603 Boudjema, N., Drouiche, N., Abdi, N., Grib, H., Lounici, H., Pauss, A., Mameri, N., 2014.
604 Treatment of Oued El Harrach river water by electrocoagulation noting the effect of the
605 electric field on microorganisms. *J. Taiwan Inst. Chem. Eng.* 45, 1564–1570.
606 <https://doi.org/10.1016/j.jtice.2013.10.006>

607 Charriau, A., Lesven, L., Gao, Y., Leermakers, M., Baeyens, W., Ouddane, B., Billon, G., 2011.
608 Trace metal behaviour in riverine sediments: Role of organic matter and sulfides. *Appl.*
609 *Geochemistry* 26, 80–90. <https://doi.org/10.1016/J.APGEOCHEM.2010.11.005>

610 Chemrouk, O., Chabbi, N., 2016. Vulnerability of Algiers Waterfront and the New Urban
611 Development Scheme. *Procedia Eng.* 161, 1417–1422.
612 <https://doi.org/10.1016/j.proeng.2016.08.603>

613 Chen, C.W., Kao, C.M., Chen, C.F., Dong, C. Di, 2007. Distribution and accumulation of heavy
614 metals in the sediments of Kaohsiung Harbor, Taiwan. *Chemosphere* 66, 1431–1440.
615 <https://doi.org/10.1016/J.CHEMOSPHERE.2006.09.030>

616 Chester, R., Stoner, J.H., 1973. Pb in Particulates from the Lower Atmosphere of the Eastern
617 Atlantic. *Nat.* 1973 2455419 245, 27–28. <https://doi.org/10.1038/245027b0>

618 Ergin, M., Yörük, R., 1990. Distribution and texture of the bottom sediments in a semi-enclosed
619 coastal inlet, the Izmit Bay from the eastern sea of Marmara (Turkey). *Estuar. Coast. Shelf Sci.*
620 30, 647–654. [https://doi.org/10.1016/0272-7714\(90\)90100-6](https://doi.org/10.1016/0272-7714(90)90100-6)

621 Esen, E., Kucuksezgin, F., Uluturhan, E., 2010. Assessment of trace metal pollution in surface
622 sediments of Nemrut Bay, Aegean Sea. *Environ. Monit. Assess.* 160, 257–266.
623 <https://doi.org/10.1007/s10661-008-0692-9>

624 Fu, F., Wang, Q., 2011. Removal of heavy metal ions from wastewaters: A review. *J. Environ.*
625 *Manage.* 92, 407–418. <https://doi.org/10.1016/J.JENVMAN.2010.11.011>

626 Gao, L., Chen, J., Tang, C., Ke, Z., Wang, J., Shimizu, Y., Zhu, A., 2015. Distribution, migration
627 and potential risk of heavy metals in the Shima River catchment area, South China. *Environ.*
628 *Sci. Process. Impacts* 17, 1769–1782. <https://doi.org/10.1039/c5em00156k>

629 Gao, L., Wang, Z., Shan, J., Chen, J., Tang, C., Yi, M., Zhao, X., 2016. Distribution characteristics
630 and sources of trace metals in sediment cores from a trans-boundary watercourse: An example
631 from the Shima River, Pearl River Delta. *Ecotoxicol. Environ. Saf.* 134, 186–195.
632 <https://doi.org/10.1016/j.ecoenv.2016.08.020>

633 Gao, X., Zhou, F., Chen, C.T.A., Xing, Q., 2015. Trace metals in the suspended particulate matter
634 of the Yellow River (Huanghe) Estuary: Concentrations, potential mobility, contamination

- 635 assessment and the fluxes into the Bohai Sea. *Cont. Shelf Res.* 104, 25–36.
- 636 <https://doi.org/10.1016/j.csr.2015.05.005>
- 637 Guendouzi, Y., Boulahdid, M., Rouane Hacene, O., Inal, A., Boudjellal, B., Fowler, S.W., 2021.
- 638 Contamination level and ecological risk assessment of particulate trace metals in Southwestern
- 639 Mediterranean Sea. *Reg. Stud. Mar. Sci.* 46, 101876.
- 640 <https://doi.org/10.1016/j.rsma.2021.101876>
- 641 Guendouzi, Y., Soualili, D.L., Fowler, S.W., Boulahdid, M., 2020. Environmental and human
- 642 health risk assessment of trace metals in the mussel ecosystem from the Southwestern
- 643 Mediterranean. *Mar. Pollut. Bull.* 151. <https://doi.org/10.1016/j.marpolbul.2019.110820>
- 644 Guo, Y., Yang, S., 2016. Heavy metal enrichments in the Changjiang (Yangtze River) catchment
- 645 and on the inner shelf of the East China Sea over the last 150years. *Sci. Total Environ.* 543,
- 646 105–115. <https://doi.org/10.1016/j.scitotenv.2015.11.012>
- 647 Hassani, M., Saadoud, D., Chabou, M.C., Martín-Peinado, F.J., Sánchez-Marañón, M., 2019.
- 648 Spectral signs of aeolian activity around a sand-dune belt in northern Algeria. *CATENA* 182,
- 649 104175. <https://doi.org/10.1016/J.CATENA.2019.104175>
- 650 Heiri, O., Lotter, A.F., Lemcke, G., 2001. Loss on ignition as a method for estimating organic and
- 651 carbonate content in sediments: reproducibility and comparability of results, *Journal of*
- 652 *Paleolimnology*.
- 653 Hong, W.L., Latour, P., Sauer, S., Sen, A., Gilhooly, W.P., Lepland, A., Fouskas, F., 2020. Iron
- 654 cycling in Arctic methane seeps. *Geo-Marine Lett.* 40, 391–401.
- 655 <https://doi.org/10.1007/s00367-020-00649-5>
- 656 Ip, C.C.M., Li, X.-D., Zhang, G., Wai, O.W.H., Li, Y.-S., 2007. Trace metal distribution in

657 sediments of the Pearl River Estuary and the surrounding coastal area, South China. *Environ.*
658 *Pollut.* 147, 311–23. <https://doi.org/10.1016/j.envpol.2006.06.028>

659 Janaki-Raman, D., Jonathan, M.P., Srinivasalu, S., Armstrong-Altrin, J.S., Mohan, S.P., Ram-
660 Mohan, V., 2007. Trace metal enrichments in core sediments in Muthupet mangroves, SE
661 coast of India: Application of acid leachable technique. *Environ. Pollut.* 145, 245–257.
662 <https://doi.org/10.1016/j.envpol.2006.03.012>

663 Jiao, W., Ouyang, W., Hao, F., Lin, C., 2015. Anthropogenic impact on diffuse trace metal
664 accumulation in river sediments from agricultural reclamation areas with geochemical and
665 isotopic approaches. *Sci. Total Environ.* 536, 609–615.
666 <https://doi.org/10.1016/j.scitotenv.2015.07.118>

667 Khelil, N., Larid, M., Grimes, S., Le Berre, I., Peuziat, I., 2019. Challenges and opportunities in
668 promoting integrated coastal zone management in Algeria: Demonstration from the Algiers
669 coast. *Ocean Coast. Manag.* 168, 185–196. <https://doi.org/10.1016/j.ocecoaman.2018.11.001>

670 Komada, T., Burdige, D.J., Magen, C., Li, H.L., Chanton, J., 2016. Recycling of Organic Matter in
671 the Sediments of Santa Monica Basin, California Borderland. *Aquat. Geochemistry* 22, 593–
672 618. <https://doi.org/10.1007/s10498-016-9308-0>

673 Kouidri, M., Dali youcef, N., Benabdellah, I., Ghouali, R., Bernoussi, A., Lagha, A., 2016.
674 Enrichment and geoaccumulation of heavy metals and risk assessment of sediments from coast
675 of Ain Temouchent (Algeria). *Arab. J. Geosci.* 9. <https://doi.org/10.1007/s12517-016-2377-y>

676 Kristensen, E., Bouillon, S., Dittmar, T., Marchand, C., 2008. Organic carbon dynamics in
677 mangrove ecosystems: A review. *Aquat. Bot.* 89, 201–219.
678 <https://doi.org/10.1016/j.aquabot.2007.12.005>

679 Li, Y., Li, H. guan, 2017. Historical records of trace metals in core sediments from the Lianyungang
680 coastal sea, Jiangsu, China. *Mar. Pollut. Bull.* 116, 56–63.
681 <https://doi.org/10.1016/j.marpolbul.2016.12.063>

682 Lin, Q., Liu, E., Zhang, E., Li, K., Shen, J., 2016. Spatial distribution, contamination and ecological
683 risk assessment of heavy metals in surface sediments of Erhai Lake, a large eutrophic plateau
684 lake in southwest China. *Catena* 145, 193–203. <https://doi.org/10.1016/j.catena.2016.06.003>

685 Liu, S., Shi, X., Liu, Y., Zhu, Z., Yang, G., Zhu, A., Gao, J., 2011. Concentration distribution and
686 assessment of heavy metals in sediments of mud area from inner continental shelf of the East
687 China Sea. *Environ. Earth Sci.* 64, 567–579. <https://doi.org/10.1007/s12665-011-0941-z>

688 Long, E.R., Ingersoll, C.G., MacDonald, D.D., 2006. Calculation and uses of mean sediment quality
689 guideline quotients: A critical review. *Environ. Sci. Technol.*
690 <https://doi.org/10.1021/es058012d>

691 Long, E.R., MacDonald, D.D., 1998. Recommended uses of empirically derived, sediment quality
692 guidelines for marine and estuarine ecosystems. *Hum. Ecol. Risk Assess.*
693 <https://doi.org/10.1080/10807039891284956>

694 Long, E.R., Macdonald, D.D., Severn, C.G., Hong, C.B., 2000. CLASSIFYING PROBABILITIES
695 OF ACUTE TOXICITY IN MARINE SEDIMENTS WITH EMPIRICALLY DERIVED
696 SEDIMENT QUALITY GUIDELINES, *Environmental Toxicology and Chemistry.*

697 Mao, L., Liu, L., Yan, N., Li, F., Tao, H., Ye, H., Wen, H., 2020. Factors controlling the
698 accumulation and ecological risk of trace metal(loid)s in river sediments in agricultural field.
699 *Chemosphere* 243. <https://doi.org/10.1016/j.chemosphere.2019.125359>

700 Martínez-Santos, M., Probst, A., García-García, J., Ruiz-Romera, E., 2015. Influence of

701 anthropogenic inputs and a high-magnitude flood event on metal contamination pattern in
702 surface bottom sediments from the Deba River urban catchment. *Sci. Total Environ.* 514, 10–
703 25. <https://doi.org/10.1016/j.scitotenv.2015.01.078>

704 Morelli, G., Gasparon, M., Fierro, D., Hu, W.P., Zawadzki, A., 2012. Historical trends in trace
705 metal and sediment accumulation in intertidal sediments of Moreton Bay, southeast
706 Queensland, Australia. *Chem. Geol.* 300–301, 152–164.
707 <https://doi.org/10.1016/j.chemgeo.2012.01.023>

708 Morse, J.W., Luther, G.W., 1999. Chemical influences on trace metal-sulfide interactions in anoxic
709 sediments. *Geochim. Cosmochim. Acta* 63, 3373–3378. [https://doi.org/10.1016/S0016-](https://doi.org/10.1016/S0016-7037(99)00258-6)
710 [7037\(99\)00258-6](https://doi.org/10.1016/S0016-7037(99)00258-6)

711 Moushmi, K.S., Cheriyan, A.S., Cheriyan, E., Mohan, M., Chandramohanakumar, N., 2022. Trace
712 metal distribution and ecological risk assessment in the core sediments of a highly urbanized
713 tropical mangrove ecosystem, Southwest coast of India. *Mar. Pollut. Bull.* 175.
714 <https://doi.org/10.1016/j.marpolbul.2021.113163>

715 Ontiveros-Cuadras, J.F., Ruiz-Fernández, A.C., Pérez-Bernal, L.H., Raygoza-Viera, J.R., Sanchez-
716 Cabeza, J.A., 2021. Historical reconstruction of trace element concentrations and fluxes in a
717 tropical coastal lagoon (Mexican Pacific) derived from ²¹⁰Pb radiochronology. *Cont. Shelf*
718 *Res.* 213, 104315. <https://doi.org/10.1016/J.CSR.2020.104315>

719 Orani, A.M., Vassileva, E., Renac, C., Schmidt, S., Angelidis, M.O., Rozmaric, M., Louw, D.,
720 2019. First assessment on trace elements in sediment cores from Namibian coast and pollution
721 sources evaluation. *Sci. Total Environ.* 669, 668–682.
722 <https://doi.org/10.1016/j.scitotenv.2019.03.059>

723 Pattan, J.N., Parthiban, G., Amonkar, A., 2019. Productivity controls on the redox variation in the

724 southeastern Arabian Sea sediments during the past 18 kyr. *Quat. Int.* 523, 1–9.
725 <https://doi.org/10.1016/j.quaint.2019.05.034>

726 Ranjan, P., Ramanathan, A.L., Kumar, A., Singhal, R.K., Datta, D., Venkatesh, M., 2018. Trace
727 metal distribution, assessment and enrichment in the surface sediments of Sundarban
728 mangrove ecosystem in India and Bangladesh. *Mar. Pollut. Bull.* 127, 541–547.
729 <https://doi.org/10.1016/J.MARPOLBUL.2017.11.047>

730 Romano, E., Bergamin, L., Celia Magno, M., Pierfranceschi, G., Ausili, A., 2018. Temporal
731 changes of metal and trace element contamination in marine sediments due to a steel plant:
732 The case study of Bagnoli (Naples, Italy). *Appl. Geochemistry* 88, 85–94.
733 <https://doi.org/10.1016/j.apgeochem.2017.05.012>

734 Salmanighabeshi, S., Palomo-Marín, M.R., Bernalte, E., Rueda-Holgado, F., Miró-Rodríguez, C.,
735 Fadic-Ruiz, X., Vidal-Cortez, V., Cereceda-Balic, F., Pinilla-Gil, E., 2015. Long-term
736 assessment of ecological risk from deposition of elemental pollutants in the vicinity of the
737 industrial area of Puchuncaví-Ventanas, central Chile. *Sci. Total Environ.* 527–528, 335–343.
738 <https://doi.org/10.1016/j.scitotenv.2015.05.010>

739 Sbarbati, C., Barbieri, M., Barron, A., Bostick, B., Colombani, N., Mastrocicco, M., Prommer, H.,
740 Passaretti, S., Zheng, Y., Petitta, M., 2020. Redox dependent arsenic occurrence and
741 partitioning in an industrial coastal aquifer: Evidence from high spatial resolution
742 characterization of groundwater and sediments. *Water (Switzerland)* 12, 1–20.
743 <https://doi.org/10.3390/w12102932>

744 Sun, Q., Liu, D., Liu, T., Di, B., Wu, F., 2012. Temporal and spatial distribution of trace metals in
745 sediments from the northern Yellow Sea coast, China: Implications for regional anthropogenic
746 processes. *Environ. Earth Sci.* 66, 697–705. <https://doi.org/10.1007/s12665-011-1277-4>

- 747 Taieb Errahmani, D., Nouredine, A., Abril-Hernández, J.M., Boulahdid, M., 2020. Environmental
748 radioactivity in a sediment core from Algiers Bay: Radioecological assessment, radiometric
749 dating and pollution records. *Quat. Geochronol.* 56.
750 <https://doi.org/10.1016/j.quageo.2019.101049>
- 751 Tomlinson, D.L., Wilson, J.G., Harris, C.R., Jeffrey, D.W., 1980. Problems in the assessment of
752 heavy-metal levels in estuaries and the formation of a pollution index.
- 753 UNEP/WHO, 1999. Identification of priority pollution hot spots and sensitive areas in the
754 Mediterranean. MAP Technical Reports Series No.124. UNEP, Athens.
- 755 Viers, J., Dupré, B., Gaillardet, J., 2009. Chemical composition of suspended sediments in World
756 Rivers: New insights from a new database. *Sci. Total Environ.* 407, 853–868.
757 <https://doi.org/10.1016/j.scitotenv.2008.09.053>
- 758 Ytreberg, E., Eriksson, M., Maljutenko, I., Jalkanen, J.P., Johansson, L., Hassellöv, I.M., Granhag,
759 L., 2020. Environmental impacts of grey water discharge from ships in the Baltic Sea. *Mar.*
760 *Pollut. Bull.* 152. <https://doi.org/10.1016/j.marpolbul.2020.110891>
- 761 Zhu, L., Liu, J., Xu, S., Xie, Z., 2017. Deposition behavior, risk assessment and source
762 identification of heavy metals in reservoir sediments of Northeast China. *Ecotoxicol. Environ.*
763 *Saf.* 142, 454–463. <https://doi.org/10.1016/j.ecoenv.2017.04.039>

764 **FIGURE CAPTIONS**

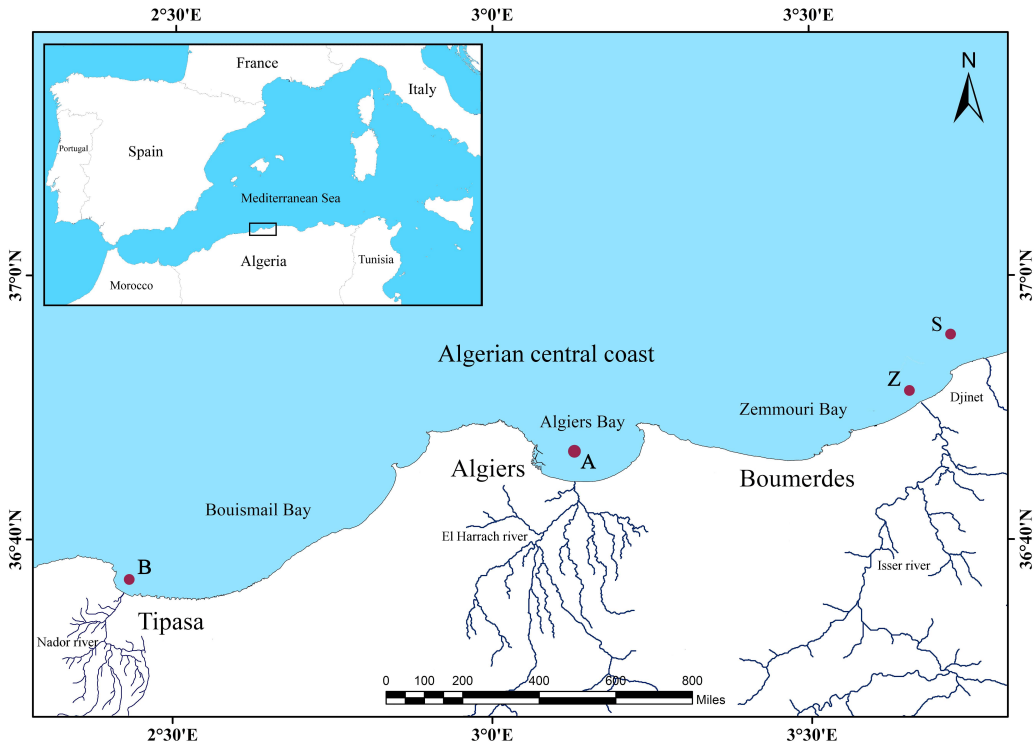
765 **Figure 1.** Map of the study area and locations of sampling sites.

766 **Figure 2.** Vertical distributions of major and trace element concentrations in cores A, B and Z
767 (concentration in mg.kg^{-1} dry weight except for Fe, Al and Na in g/kg).

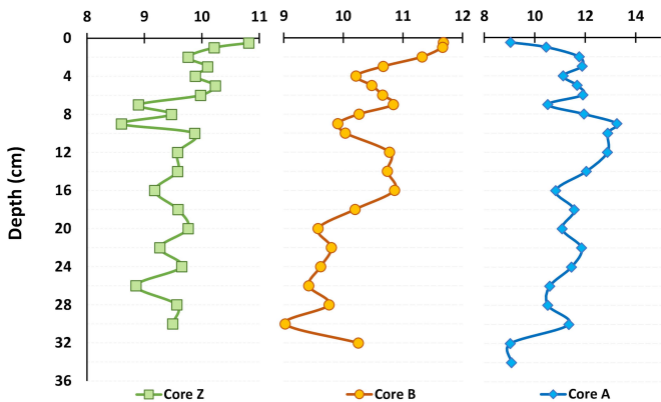
768 **Figure 3.** Vertical variations of organic matter, water and total sulfur contents in the sediment cores
769 A, B and Z of Algerian central coast. The solid lines in (b) represent the exponential curves that has
770 been linked by water content data.

771 **Figure 4.** Enrichment factors calculating for the central coast sediment.

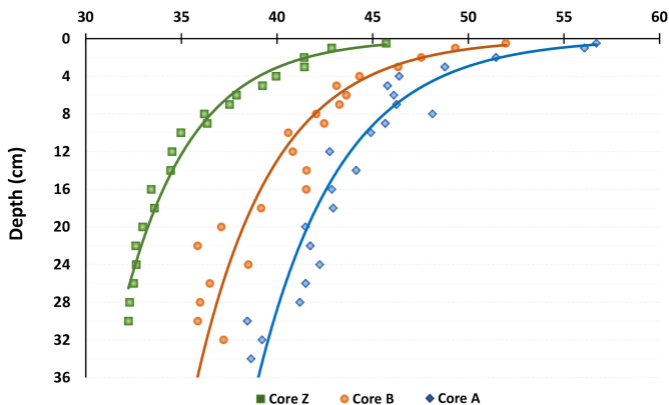
772 **Figure 5.** Results of pollution load index (PLI) and Mean sediment quality guideline quotients (Qm-
773 SQG) according to the method employed by Tomlinson et al. (1980) and Long et al. (2000),
774 respectively.



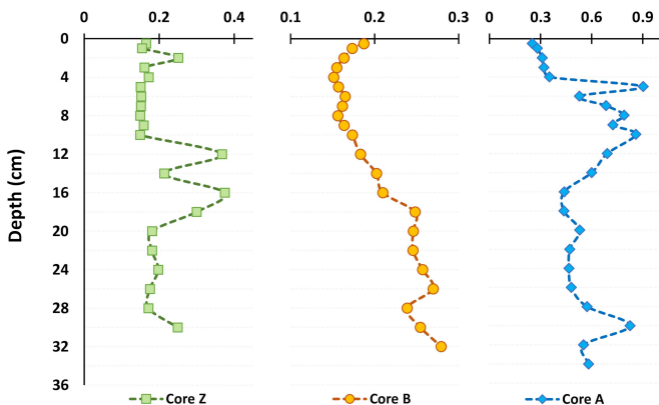
Organic Matter %

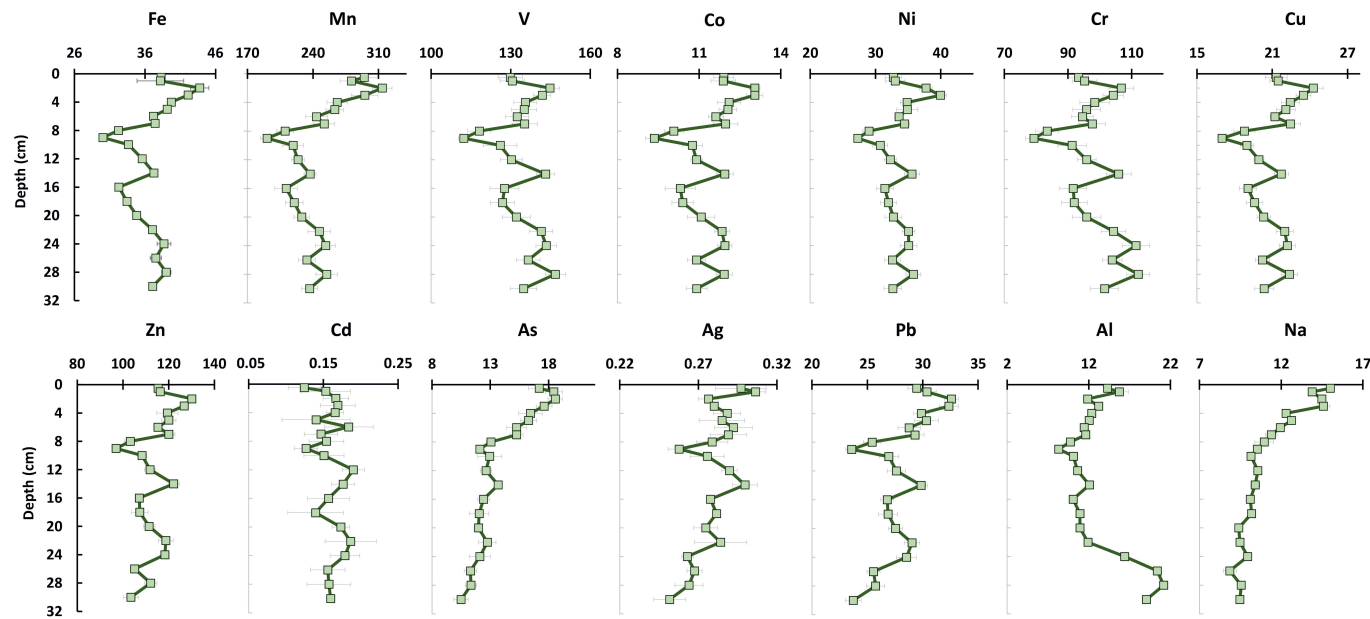
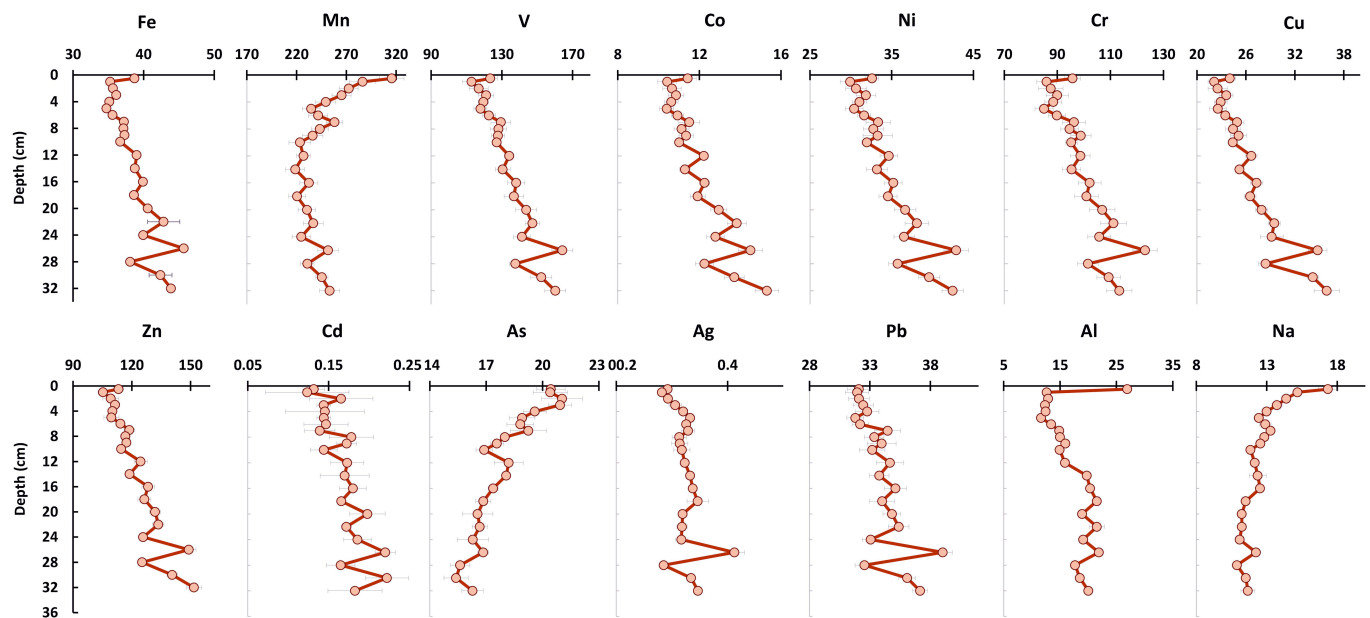
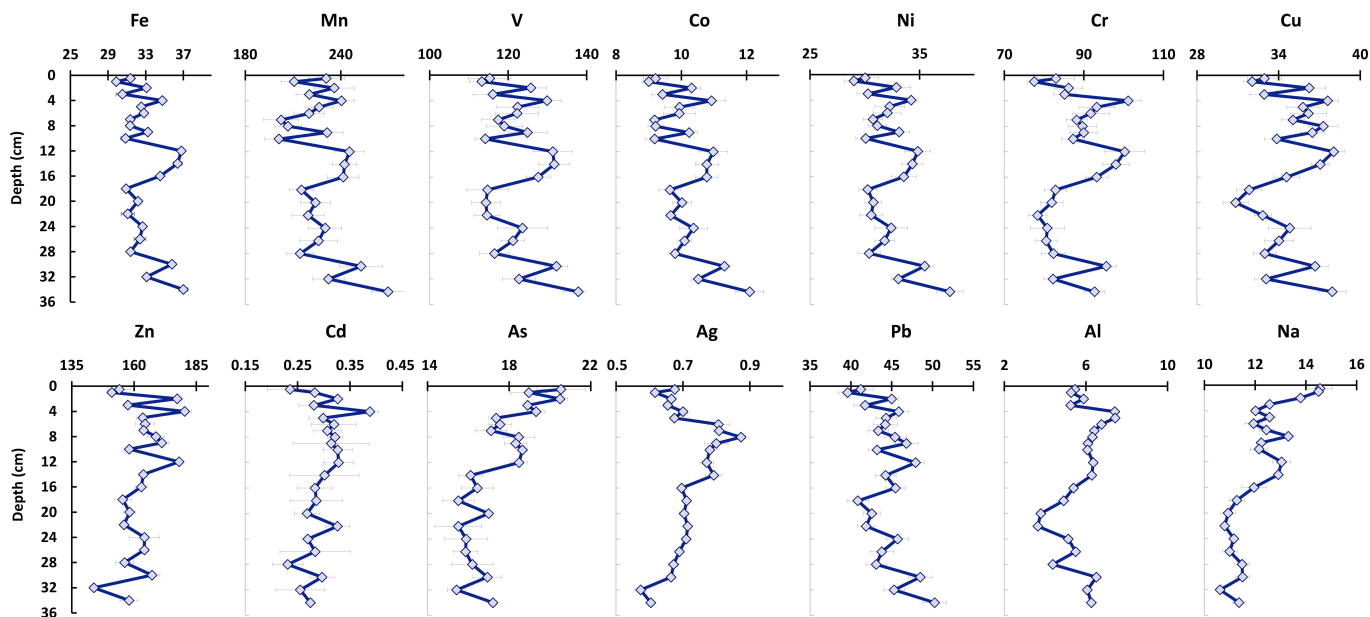


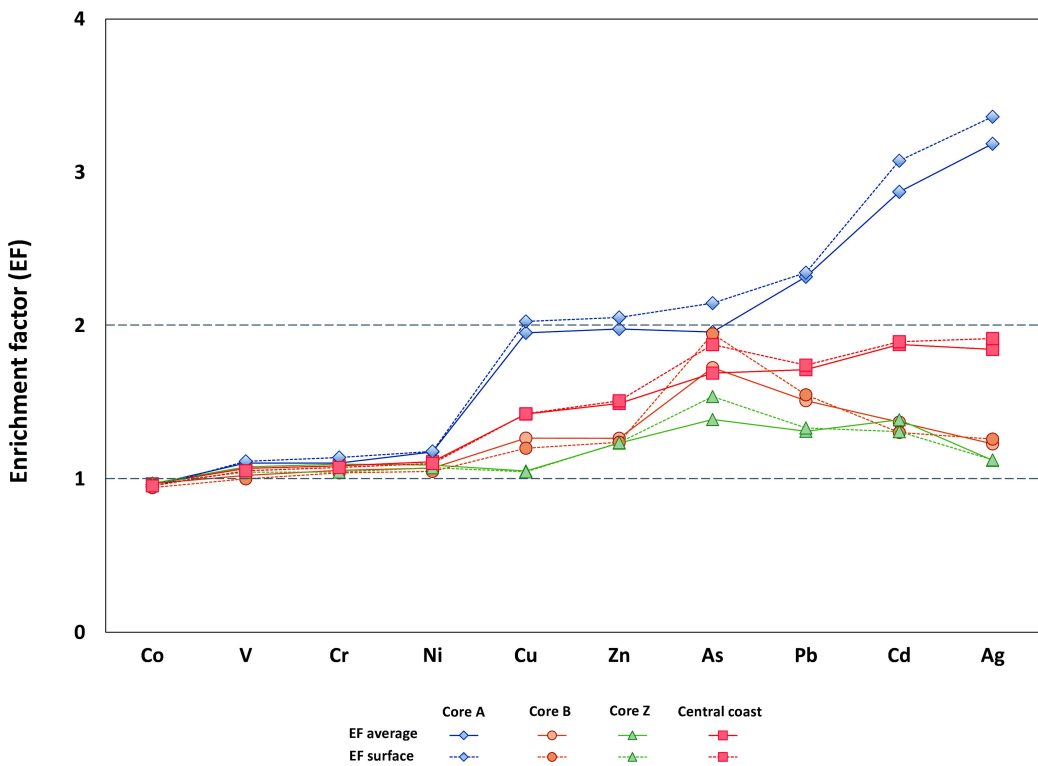
Total water %



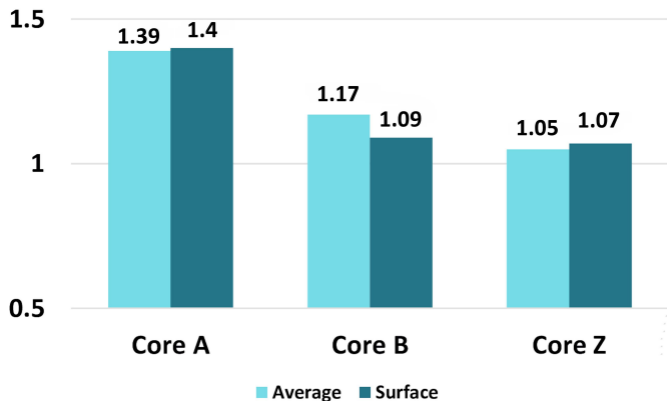
Total Sulfur %







PLI



Qm-SQGs

